Comparison of ultraviolet photoelectron spectroscopy and scanning tunneling spectroscopy measurements on highly ordered ultrathin films of hexa-*peri*-hexabenzocoronene on Au(111)

Holger Proehl,* Michael Toerker, Farid Sellam, Torsten Fritz, and Karl Leo†
Institut für Angewandte Photophysik, Technische Universität Dresden, 01062 Dresden, Germany

Christopher Simpson and Klaus Müllen
MPI für Polymerforschung, Ackermannweg 10, 55128 Mainz, Germany

(Received 25 July 2000; revised manuscript received 12 January 2001; published 25 April 2001)

Hexa-*peri*-hexabenzocoronene ($C_{42}H_{18}$, HBC) films adsorbed on the Au(111) surface were investigated by means of ultraviolet photoelectron spectroscopy (UPS) and scanning tunneling spectroscopy (STS). The results show that both methods give comparable results for the electronic structure of the occupied states, if the STS is performed at appropriate parameters. Additionally, STS gives an immediate insight into the unoccupied states. The highest occupied state of multilayer films is found 1.3–1.4 eV below the Fermi levels and the lowest unoccupied state 1.8 eV above the Fermi level. The resulting transport gap is compared to optical absorption measurements. Work-function changes of -0.8 eV indicate an interface dipole, i.e., vacuum level alignment does not occur at the HBC-Au interface. Compared to UPS, the voltage range of the STS measurements is limited to prevent sample damage.

DOI: 10.1103/PhysRevB.63.205409 PACS number(s): 73.61.Ph, 68.37.Ef, 79.60.−i, 81.15.Hi

I. INTRODUCTION

The knowledge and understanding of the metal-organic interface plays a significant role in the further development and improvement of organic and molecular electronics. For instance, injection barriers and therefore operational voltages of electronic and optoelectronic devices like organic light-emitting devices (OLED's) are influenced by the energy-level alignment at the contacts.[1] In particular, highly ordered thin molecular films can provide a deeper insight into the physical processes at those interfaces. Consequently, the mechanisms of growth as well as the optical and electronic properties of certain model compounds on various metallic and semiconducting substrates have been studied in detail.[2–7] A large number of ultraviolet photoelectron spectroscopy (UPS) investigations of the metal-organic interface were already reported.[8–11] Large flat hydrocarbons like hexa-*peri*-hexabenzocoronene (HBC) are useful as relatively simple model compounds which have been shown to grow in large ordered domains and which have interesting electronic properties.[12] Among those, HBC is especially interesting because of its high symmetry. The growth of HBC and derivatives on different substrates like highly oriented-pyrolytic graphite (HOPG) and metal dichalcogenides,[13,14] as well as scanning tunneling spectroscopy measurements of self-assembled alkyl-substituted HBC in solution,[15] have already been reported. A very high charge carrier mobility was observed for self-assembled alkyl-substituted HBC stacks in the stack direction.[16] Recently, a UPS study of the electronic structure of rather thick evaporated HBC films grown on different substrates was published.[17] Here we report a combined UPS/STS (scanning tunneling spectroscopy) study of the interface between highly ordered HBC and the Au(111) surface, and the nature of interaction at this interface.

II. EXPERIMENT

The organic films were deposited under ultrahigh-vacuum (UHV) conditions by evaporation from low-flux sublimation cells at a cell temperature of 690 K and a vapor pressure of 3×10^{-8} mbar. The evaporation was done after a thorough degassing of the cells at ~600 K for 12 h. The deposition rate was about 0.5 (ML) per minute, and was calibrated via scanning tunneling microscopy (STM) for thin films and via quartz microbalance for thicker films. During and after film deposition, the substrate was kept at room temperature. For every measurement, a different film was deposited onto the gold crystal, which was previously prepared by several sputter/annealing cycles (600-eV Ar^+ ions, 870 K) to obtain an acceptable level of surface cleanliness [controlled by the observation of C 1*s* and O 1*s* core-level spectra in x-ray photoemission spectroscopy (XPS)] and to exhibit the typical $(22\times\sqrt{3})$ surface reconstruction. The ordering of the films was checked by low energy electron diffraction (LEED).

Ultraviolet photoelectron spectroscopy measurements were carried out in a separate chamber at a base pressure of 1×10^{-10} mbar, using a hemispheric analyzer (VG Clam2) equipped with radiation sources for UV and x-ray (He *I*, 21.2 eV, and Mg-$K\alpha$, 1253.6 eV). For He *I* excitation, the electron energy distribution curves (EDC's) were obtained at a 2-eV analyzer pass energy, which implies an analyzer resolution of 50 meV. For the work-function measurements, the sample was held at −3-V bias to clear off the detector work function. The peak onsets, and the high-binding-energy cutoffs, respectively, were determined by an intersection of the tangents of the peak and the (background) base line, with an overall error of estimated ±100 meV.

Scanning tunneling spectra were obtained with a UHV-STM system (Omicron STM/AFM) at a fixed tip-sample separation. The bias voltage V was applied in a way that positive voltages mean electron-tunneling into unoccupied states of the sample. When recording the $I(V)$ curves, the actual scan was stopped, the tip was moved to the desired position, and after a delay of 2.5 ms the feedback loop was switched off and a voltage ramp (a typical step size 20 mV

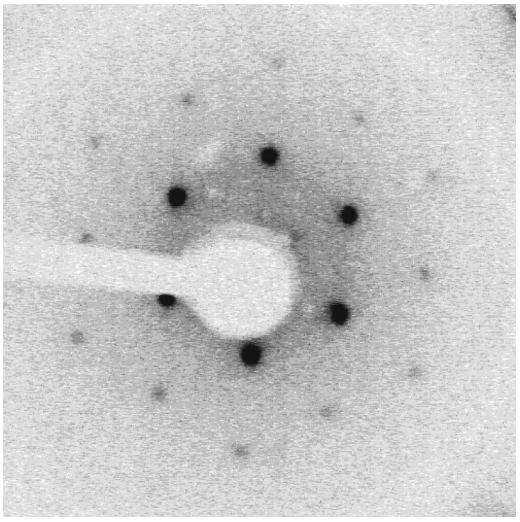

FIG. 1. Typical LEED pattern of thin HBC films, taken at a 24-eV beam energy. Shown is the example of a 2-ML-thick film. The simplicity of the LEED pattern indicates a single-domain growth mode.

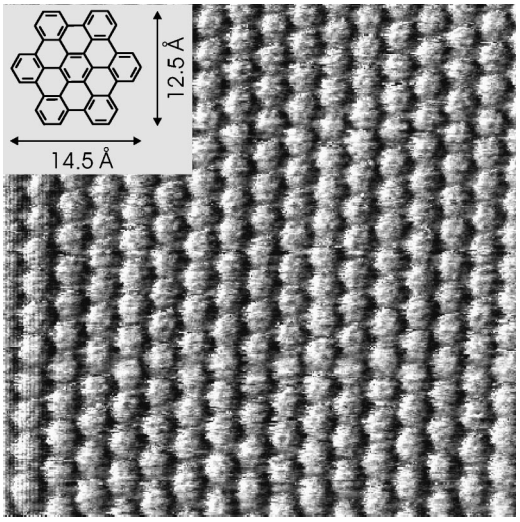

FIG. 2. STM (current-) image of a 2–3-ML HBC on a Au(111) film ($U=1.0$ V; $I=0.2$ nA; 20×20 nm^2; not drift corrected, unfiltered raw data). The inset shows the structural formula and the van der Waals dimensions of the HBC molecule.

per 0.2 ms) was applied. With completion of this procedure, the interrupted scan was continued. The measurement range of the tunnel current preamplifier was ±50 nA, to safely avoid overmodulation at the ends of the $I(V)$ curves. The recorded $I(V)$ curves at one position were averaged over at least ten successive ramp repetitions, and the derivatives were calculated numerically. To avoid singularities in the normalized derivative $(dI/dV)/(I/V)$ at $V=0$, we added a small constant to the value of I/V following the procedure of Ref. 18. The W tips used were electrochemically etched in NaOH solution, and rinsed in distilled water and pure ethanol. After transferring the tips into the vacuum system and before every measurement, the tips were annealed at about 870 K and sputtered with 2-keV Ar^+ ions to remove any contamination. For the absorption measurements, a Shimadzu spectrophotometer (UV-3101PC) was utilized.

III. RESULTS AND DISCUSSION

A. UPS

The LEED images (Fig. 1 at 2-ML HBC coverage) show a simple characteristic sixfold diffraction pattern according to a lattice constant of 14.7 ± 0.5 Å for monolayers which would correspond to a commensurate $(\sqrt{27}\times\sqrt{27})R30°$ structure with respect to an unreconstructed Au(111) surface. A more detailed analysis, including scanning tunneling microscopy investigations, yields a point-on-line coincident growth mode, with the important observation that the adsorption of HBC on the Au(111) surface changes (weakens) its surface reconstruction. An annealing of HBC multilayers causes desorption of HBC until the HBC monolayer, but up to a temperature of 870 K the LEED pattern of this first monolayer did not show a remarkable change or intensity loss. With STM the mutual molecular alignment could be observed; it exhibits a hexagonally close-packed structure of apparently flat-lying molecules with $p6mm$ symmetry, as shown in Fig. 2 for a 2–3-ML HBC film. This layered growth mode, with defect-free domain sizes of about 100×100 nm^2, is entirely different from the bulk crystal structure,[19] comparable with the structures found on weak interacting substrates like MoS_2 or graphite,[13] with the exception of the unusually large lattice constant of the first layer. Thicker films show a compression of the lattice constant down to 13.7 ± 0.8 Å for 6-ML films. The detailed study of the growth of ultrathin HBC films on Au(111) single-crystal surfaces will be given elsewhere.[20]

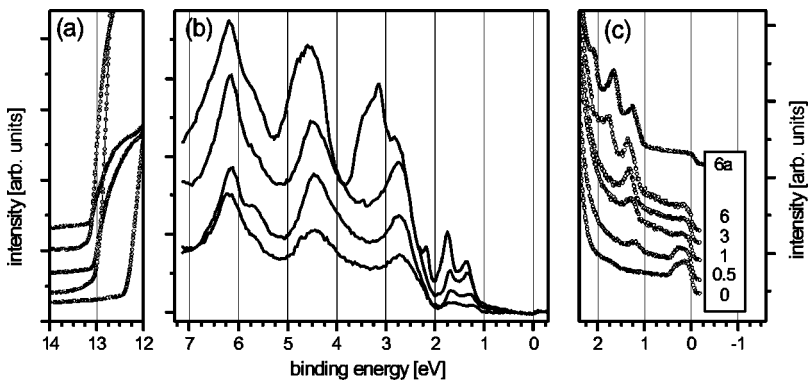

FIG. 3. UP spectra of HBC on Au(111) for increasing film thickness from 0 ML (bare Au) to 6 ML, labeled by 0–6. (a) He I cutoff in 0° emission. (b) 30° emission difference EDC's, normalized for the intensities in the Fermi plateau range. By removing the background (mainly caused by the inelastic scattered electrons from the gold) the HBC-induced features appear more pronounced. (c) Valence UP spectra in 0° emission. For comparison, the 30° EDC for the thickest layer is shown also (indicated as $6a$).

TABLE I. Coverage-dependent position of the first occupied valence state of the HBC/Au(111) system for different investigation methods. For STS measurements, the results at 3-ML coverage show agreement with the UPS data. The values in brackets correspond to the respective peak onsets. (VL is the vacuum level and FL is the Fermi level)

		UPS		STS
Film thickness (ML)	Φ (eV)	First val. state resp. FL (eV)	First val. state resp. VL (eV)	First val. state resp. FL (eV)
0.5–1	4.6	1.25 (1.1)	5.9 (5.7)	n.a.
3	4.5	1.35 (1.1)	5.9 (5.6)	1.4 (1.2)
6	4.5	1.35 (1.1)	5.9 (5.6)	n.a.

In Fig. 3, the He *I* EDC of a clean Au(111) surface shows the known peak of a Shockley surface state at a binding energy of $E_B = 0.4$ eV (Ref. 21) (relative to the Fermi level) which is smeared out to higher kinetic energies due to the rather large acceptance angle of the spectrometer of about 8°. This peak disappears with increasing coverage of HBC, while an interesting feature appears, centered at $E_B = 1.25$ eV. Its position moves slightly at higher coverage to a higher binding energy of 1.35 eV at 6-ML coverage (compare Table I). This difference between the first and the subsequent layers of HBC can be understood by the possibility of filling the photogenerated holes of the first HBC layer with electrons from the Au valence band, a process which is suppressed for subsequent layers. This different behavior of the first two layers, the observed changes of the Au(111) surface reconstruction due the absorption of HBC, and the fact that thermal desorption of a HBC monolayer from the Au(111) surface is impossible, lead to the conclusion of a relatively strong interaction at the HBC-Au(111) interface.

To enhance the surface sensitivity, EDC's of the 30° emission were also recorded. In the case of very thin films, the evaluation of the difference spectra of EDC's of bare Au and Au covered by HBC (normalized for the intensities at an energy within the Fermi plateau) can possibly give an insight into the adsorbate-induced changes by reducing the background which is mainly caused by the Au. Interesting details were found: While a second feature is obtained at $E_B \sim 1.7$ eV for all coverages (rather weak at 0.5 ML), in the 0° difference spectrum (not shown here) this feature appears only at the highest coverage of 6 ML. Conversely, an additional peak at $E_B \sim 2.2$ eV arises in the difference spectra of 30° emission only at a coverage of 6 ML, but is permanently present in the 0° spectra. For the 30° spectra the high-binding-energy features at 2.7, 4.5, and 6.3 eV are much broader than the first three. In Table II the photoemission data of these higher occupied states are summarized.

Because of the interaction between the Au valence-band electrons with the HBC molecules of the first layer, a broadening of the HBC states and a shift of the energetic levels occur. The intermolecular interaction between the HBC molecules within a layer is rather small. Due to the layer-by-layer growth, influences on the spectra by solid-state effects like *intermolecular* polarization and relaxation are expected to be enhanced for thicker films, with a pronounced formation of molecular stacks (the distance of layers ~3.5 Å, compared with the film lattice constant of ~14 Å). The slight changes in the spectra of the 6-ML film, with the loss of the different angular dependencies of the first three valence states as can be seen in Fig. 3 and Table II, seems to point in this direction, but other effects, such as changes of the morphology of thicker films, which would lower the symmetry of the film, have to be taken into account as well. A relaxation of the structure of the film toward the crystal structure could be accompanied by a tilting of the molecules out of the layer plane. It is perhaps noteworthy to remark that Keil *et al.*[17] reported only one unresolved feature (of about 1.1-eV width) at $E_B = 1.8$ eV for 10-nm-thick unordered HBC films on polycrystalline gold. A different surrounding of each molecule would lead to a broadening of the first three valence states, so only a broad feature is visible instead. This could further support the expectation mentioned above, although their lower-energy resolution of 0.2 eV has to be considered.

The different lengths of the EDC's shown in Fig. 3(a) indicate a reduction of the work function Φ by 0.7 eV down to 4.6 ± 0.1 eV after 0.5–1-ML HBC deposition, as compared to $\Phi = 5.3$ eV for clean Au(111), caused by interfacial dipole moments. This value increases only slightly at higher HBC depositions, as listed in Table I. The interface dipole is the result of charge transfer processes at the HBC-Au interface; therefore, no vacuum level alignment occurs. The difference Δ of the vacuum levels has the amount of $\Delta = E^k_{\min}(\text{film}) - E^k_{\min}(\text{Au}) = -0.8$ eV for the thickest films (also see Fig. 7). A similar value of $\Delta = -1$ V can be calculated from the re-

TABLE II. Higher occupied valence states of HBC on Au(111) as measured by UPS for different film thicknesses. In normal emission (0°) the occurrence of the fourth and fifth valence states of the thinner films is concealed by the strong emission from the gold *d* bands. The values were obtained by evaluation of the 30° emission difference spectra, and are marked with (*). At 6-ML coverage, the fourth valence state splits into two parts, and a large shoulder on the high-binding energy side appears. The values in brackets correspond to the respective peak onsets. [Features indicated by * (†) are not visible in 0° (30°) emission.]

Film thickness (ML)	Second val. state resp. FL (eV)	Third val. state resp. FL (eV)	Fourth val. state resp. FL (eV)	Fifth val. state resp. FL (eV)
0.5–1	1.65 (1.5)*	2.25 (2.0)†	2.7*	4.45*
3	1.7 (1.6)*	2.25 (2.0)†	2.7*	4.45*
6	1.75 (1.6)	2.2 (2.1)	2.8	4.5

ported work function value $\Phi = 4.1$ eV for 10-nm HBC films on polycrystalline Au,[17] assuming a work function of $\Phi = 5.1$ eV for the bare polycrystalline Au. The occurrence of interfacial dipoles has often been observed at metal-organic interfaces, and was already discussed in detail.[22] (and references therein)

The binding energy of the first valence state of the solid film[23] with respect to the vacuum energy level, $I_p \sim 5.9$ eV (peak-center) is unaffected by the film thickness (as can be calculated from the values in Table I with the work function of the film). A comparison of the most prominent features of the EDC with the UP spectra of the HBC molecule in the gas phase [first vertical ionization potential $I_v(\text{gas}) = 6.8$ eV (Refs. 24 and 25)] yields an energetic shift in the UP spectra. A value of $\Delta E = I_v(\text{gas}) - I_p(\text{film}) \sim 1.1$ eV can be estimated for the thickest film, corresponding to a relative shift of the peak centers. The observed value lies in the region of relaxation energies reported for large aromatic hydrocarbons like $\Delta E_R = 1.15$ eV for polycrystalline tetracene films,[26] but a further relaxation for thicker films is likely to occur.[17]

The carbon 1*s* peak observed in the x-ray photoemission spectra (not shown here) for 1 ML was found at $E_B = 284.3$ eV, and its position did not change significantly at higher coverage; hence there is no indication for energy level bending in the thickness region investigated here. Special attention was paid to check whether organic films are damaged by the alternating structural (LEED) and spectroscopic (UPS, XPS) investigation methods. It was found that the photoemission spectra before and after recording a LEED image (with an increased electron radiation time up to about 4 min) do not exhibit any changes. Therefore, the radiation damage by electrons is negligible. Likewise, radiation damage by either x rays or UV light were not visible in a (quality) difference of LEED images taken before and after photon irradiation, even when those were extended up to 3 h. We can conclude that highly ordered HBC layers on Au(111) present an exceptionally stable model system.

B. STS

While UPS and XPS represent *integral* investigation methods, locally resolved information about the electronic structure of an adsorbate can be provided by scanning tunneling spectroscopy. However, for meaningful STS measurements one has to obey certain constraints: First, in order to make sure that the spectra characterize an *intact* molecule on the *surface*, the STM images taken before and after the spectroscopy should not reveal any differences. Second, the spectroscopy data taken repeatedly at one point should exhibit identical features. As a general rule, the accessible voltage range is rather limited in STS, due to the increased likelihood of film damage by the high electric field at elevated voltages. Thus the amount of reliable STS data is considerably reduced. At room temperature, the molecules are usually mobile, so only molecules embedded in closed films or large islands can be investigated.

For the system investigated here, the most reliable and reproducible STS data were recorded at relatively large tunneling distances, which were defined by a bias voltage of 1.3 V and a tunneling current setpoint of 0.1 nA (during image recording, and before switching off the feedback loop), corresponding to a tunneling resistance of $R = 13\ \text{G}\Omega$. Those conditions represent the imaging limit. In the spectroscopy voltage range of $(-2 - +2)$ V, maximum currents of about 1–8 nA were drawn. We plot the normalized derivative $(dI/dV)/(I/V) = d \ln I / d \ln V$ of the tunneling current I versus the applied bias voltage V (the so-called spectroscopy plot), which is related to the density of states.[27] A normalization of the differential conductivity dI/dV is advisable for an appropriate evaluation of the tunneling spectra, especially if larger voltage ranges are covered. In this case small features in the differential conductivity dI/dV can become invisible due to the large increase in the differential conductivity itself for the higher voltages (as it can be seen in Figs. 4 and 5). Different approaches of density-of-states (DOS) deconvolution have also been discussed.[28,29] On the other hand, not only the peak visibility but also the peak position can be strongly influenced by the normalization procedure. This effect was analyzed extensively by Lang.[28] Nevertheless, here we concentrate on an analysis of the normalized derivatives. Other studies confirm that the normalized derivative is also suitable for a characterization of organic adsorbate layers.[30,31]

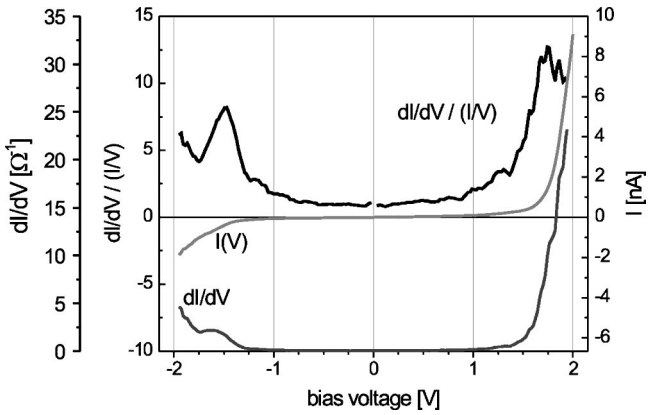

FIG. 4. Differential conductivity dI/dV and normalized dI/dV curves of a 2–3-ML-thick HBC film on Au(111), obtained numerically from the averaged $I(V)$ curves (12 repetitions). The curves were measured at a large tunneling gap for different positions, and no lateral dependence was found. A pronounced feature around $V = -1.4$ V appears in the normalized dI/dV curve. This feature is visible in the dI/dV curve too, but is slightly shifted. The feature around 1.8 V is visible only in the normalized derivative.

In the investigation of 2–3-Mo-thick films at this large tip-sample separation (Fig. 4), the most pronounced feature appears at a bias voltage of -1.4 V in the normalized derivative, corresponding to the first occupied state (HOMO).[32] This feature is visible in the dI/dV curve too. Thus in STS the HOMO feature is found at the same energetic position $(E_B = 1.4\ \text{eV})$ as in UPS. This is the expected result, because in both methods the DOS of a molecular film on a surface is probed, and for large tip-sample separations the effects of the local (on a molecular scale) variations of the DOS as well as of the tip-molecule interactions should vanish. At a positive substrate bias, another strong feature can be seen around 1.8

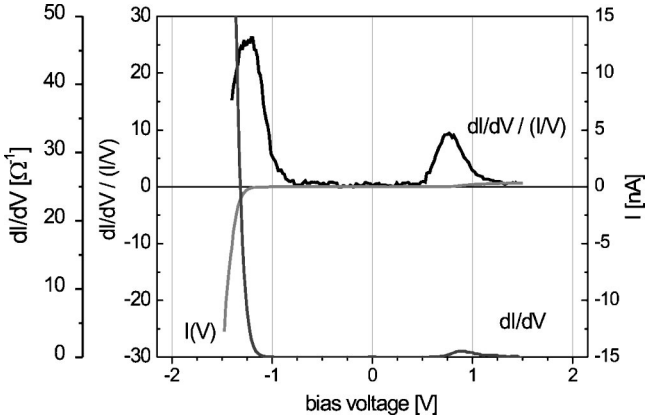

FIG. 5. Differential conductivity dI/dV and normalized dI/dV curves of a 2–3-ML-thick HBC film on Au(111), obtained numerically from the averaged $I(V)$ curves (12 repetitions). The curves were measured at a small tunneling distance. The feature around 0.8–0.9 V is visible in both the dI/dV and spectroscopy plots. The feature at negative voltages is hidden in the dI/dV curve by its large ascension.

V, at the end of the accessible voltage range (before sample damage would occur). However, this feature appears only in the normalized derivative, not in the simple derivative. To ensure that this peak is not caused by the normalization procedure itself, we compare this with optical measurements.

From absorption measurements (see Fig. 6) of thicker HBC films (~5 nm), we determined the optical gap to E_G^{opt} ~2.8 eV, taken from the onset of the (energetically) lowest absorption band. If we compare this optical gap of 2.8 eV with the gap of ~3.2 eV yielded from the peak distance in STS measurements, we obtain an energetic difference of 0.4 eV, well within the energetic region where the exciton binding energy[33] of large hydrocarbons is expected.[34] Therefore, the results obtained from the STS measurements are verified by the results of the optical measurements.

Quite differently from the UPS measurements, where no local interaction between sample and spectrometer was con-

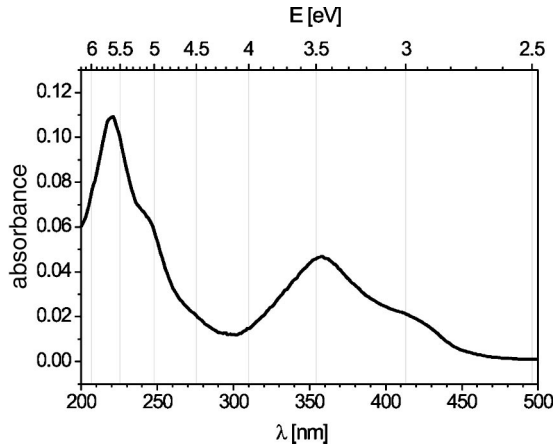

FIG. 6. Absorbance (optical density) spectrum of a ~5-nm-thick (polycrystalline) HBC film on quartz glass at room temperature. The onset position of the energetically lowest absorption band leads to an optical gap of ~2.8 eV in the crystalline phase.

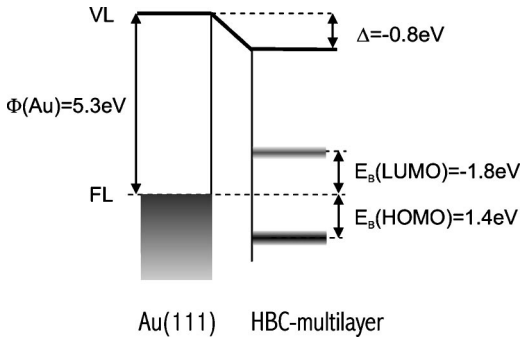

FIG. 7. Proposed interfacial energy-level diagram of the HBC-Au(111) interface for multilayer coverages.

sidered, in STS the probe itself can strongly influence the electronic properties of the sample under investigation. This is especially true for small tip-sample distances. To give an example, if the tunneling resistance is largely decreased, the spectrum seems to be compressed, i.e., the peaks are now closer to the origin, and the spectrum appears more symmetric, as the curve in Fig. 5 indicates (in this case, the tunneling resistance, which defines the tunneling distance, is reduced to $R=5\ \mathrm{G}\Omega$, while a maximum current of -20 nA was drawn at -1.5 V). The origin of this behavior is the largely increased interaction of the tip with the molecule. Interference effects become important,[35] and the high electric field can influence the electronic states. Additionally, due to its polarizability, the molecule can be lifted from the surface. One could say that the tunnel junction is now dominated by tip-molecule interaction effects. Alternatively, it is feasible that due to the small tunneling gap a molecule becomes trapped underneath the tip. This explanation is based on the observation that the strongest increase of the $I(V)$ curve now appears for negative voltages, compared to the case of larger tunneling gaps. However, one has to keep in mind that the STM images themselves, taken before and after the spectroscopy, remained unchanged. Therefore, we have to assume that the additional molecule stems either from other sample areas or from mobile molecules on the surface, as always present at room temperature.[36,37]

Monolayer films of HBC on Au(111) exhibit a special growth mode as described in the Sec. III A. These monolayer films are very difficult to image in STM; therefore, no reliable STS data, which fulfill the criteria described above, can be presented here.

For films thicker than 5 ML, the film morphology changes into small crystallites while trying STS measurements, even at smaller voltage intervals of about $(-1.5$–$1.5)$ V, probably due to the relaxation of the stress caused by the enforced metastable layered growth of the HBC films on gold.

IV. SUMMARY AND CONCLUSION

We have shown that UPS and STS give comparable results for the electronic structure of the Au-HBC interface for films up to 3-ML thickness and large tip-sample separations. In other words, in large-distance STS the local density of states is reproduced, as in the UPS data, while in the small

separation limit the tunneling current seems to be dominated by tip-molecule interaction effects, and hence the tunneling spectra do not represent the local density of states of the molecular film. In Fig. 7 the energy-level alignment at the HBC-Au(111) interface is summarized: The binding energy of the first valence state of 1.3–1.4 eV (with respect to the Fermi level) can be reproduced by UPS and STS. The binding energy with respect to the vacuum energy level, $I_p \sim 5.9\,\mathrm{eV}$ (by UPS) is independent of the film thickness. A misalignment $\Delta = -0.8\,\mathrm{eV}$ of the vacuum levels of the metal and organic overlayers was measured, corresponding to an interface dipole. The position of the first unoccupied HBC-related state is proposed to be $E_B = -1.8\,\mathrm{eV}$ for multilayer coverages. In the thickness region investigated, indication for energy-level bending was found neither in the ultraviolet nor in the x-ray photoelectron spectra.

ACKNOWLEDGMENTS

H. P. acknowledges the ''Institut für Oberflächen und Mikrostrukturphysik,'' especially the group of C. Laubschat, for the opportunity to use the photoemission spectrometer, and their member's assistance in carrying out the photoemission spectroscopy measurements. Thanks also to S. Mannsfeld and R. Nitsche for helpful discussions. Part of this work was supported by the ''Bundesministerium für Bildung, Wissenschaft, Forschung und Technologie'' under Grant No. 13N7169, and by the ''DFG-Graduiertenkolleg Sensorik.''

*Electronic address: proehl@iapp.de
†URL: www.iapp.de

[1] J. Blochwitz, M. Pfeiffer, T. Fritz, and K. Leo, Appl. Phys. Lett. **73**, 729 (1998).
[2] T. J. Schuerlein, A. Schmidt, P. A. Lee, K. W. Nebesny, and N. R. Armstrong, Jpn. J. Appl. Phys. **34**, 3837 (1995).
[3] C. Seidel, J. Poppensieker, and H. Fuchs, Surf. Sci. **408**, 223 (1998).
[4] K. Glöckler, C. Seidel, A. Soukopp, M. Sokolowski, E. Umbach, M. Böhringer, R. Berndt, and W. Schneider, Surf. Sci. **405**, 1 (1998).
[5] T. Fritz, *Molecular Architecture in Heteroepitaxially Grown Organic Thin Films* (Wissenschaftlicher Fachverlag, Dresden, 1999).
[6] T. Schmitz-Hübsch, F. Sellam, R. Staub, M. Törker, T. Fritz, C. Kübel, K. Müllen, and K. Leo, Surf. Sci. **445**, 358 (2000).
[7] T. Schmitz-Hübsch, T. Fritz, F. Sellam, R. Staub, and K. Leo, Phys. Rev. B **55**, 7972 (1997).
[8] I. Hill, A. Rajagopal, A. Kahn, and Y. Hu, Appl. Phys. Lett. **73**, 662 (1998).
[9] G. Koller, R. I. Blyth, S. A. Sardar, F. P. Netzler, and M. G. Ramsay, Appl. Phys. Lett. **76**, 927 (2000).
[10] S. C. Veenstra, U. Stalmach, V. V. Krasnikov, G. Hadziioannou, H. T. Jonkman, A. Heeres, and G. A. Sawatzky, Appl. Phys. Lett. **76**, 2253 (2000).
[11] R. Schlaf, P. G. Schroeder, M. W. Nelson, B. A. Parkinson, C. D. Merrit, L. A. Crisafulli, H. Murata, and Z. H. Kafafi, Surf. Sci. **450**, 142 (2000).
[12] F. Dietz, N. Tyutyulkov, G. Madjarova, and K. Müllen, J. Phys. Chem. B **104**, 1746 (2000).
[13] U. Zimmermann and N. Karl, Surf. Sci. **268**, 296 (1992).
[14] N. Karl and C. Günther, Cryst. Res. Technol. **34**, 243 (1999).
[15] A. Stabel, P. Herwig, K. Müllen, and J. Rabe, Angew. Chem. **107**, 1768 (1995).
[16] A. V. de Craats, J. Warman, A. Fechtenkötters, J. D. Brandt, M. Harbison, and K. Müllen, Adv. Mater. **11**, 1469 (1999).
[17] M. Keil, P. Samori, D. A. dos Santos, T. Kugler, S. Stafström, J. Brandt, K. Müllen, J. Bredas, J. Rabe, and W. Salaneck, J. Phys. Chem. B **104**, 3967 (2000).
[18] M. Prietsch, A. Samsavar, and R. Ludeke, Phys. Rev. B **43**, 11 850 (1991).
[19] R. Goddard, M. W. Haenel, W. C. Herndon, C. Krüger, and M. Zander, J. Am. Chem. Soc. **117**, 30 (1995).
[20] F. Sellam, T. Schmitz-Hübsch, M. Toerker, H. Proehl, K. Müllen, and K. Leo, Surf. Sci. **478**, 113 (2001).
[21] S. D. Kevan and R. H. Gaylord, Phys. Rev. B **36**, 5809 (1987).
[22] H. Ishii, K. Sugiyama, E. Ito, and K. Seki, Adv. Mater. **11**, 605 (1999).
[23] As this valence state is not identical to the highest occupied molecular orbital (HOMO) of a single molecule but is somehow related to it, we will call this state HOMO for short in the following. For the same reason we will also call the first unoccupied state of the solid film LUMO because it is related to the first unoccupied molecular state of an isolated molecule.
[24] W. Hendel, Z. Khan, and W. Schmidt, Tetrahedron **42(4)**, 1127 (1986).
[25] E. Clar and W. Schmidt, Tetrahedron **33**, 2093 (1977).
[26] *Photoemission in Solids II*, edited by L. Ley and M. Cardona (Springer-Verlag, Berlin, 1979), Chap. 5.
[27] R. Feenstra, J. Stroscio, and A. Fein, Surf. Sci. **181**, 295 (1987).
[28] N. Lang, Phys. Rev. B **34**, 5947 (1986).
[29] V. A. Ukraintsev, Phys. Rev. B **53**, 11 176 (1996).
[30] T. W. Odom, J.-L. Huang, P. Kim, M. Ouyang, and C. M. Lieber, J. Mater. Res. **13**, 2380 (1998).
[31] H. Wang, C. Zeng, Q. Li, B. Wang, J. Yang, G. Hou, and Q. Zhu, Surf. Sci. **442**, L1024 (1999).
[32] As mentioned above, negative bias voltages mean positive binding energies with respect to the Fermi level.
[33] The exciton binding energy is obtained by the difference between the optical gap (onset of absorption) and the transport gap (onset of photoconductivity).
[34] E. A. Silinsh and V. Cápec, *Organic Molecular Crystals* (AIP, New York, 1994).
[35] P. Sautet and C. Joachim, Ultramicroscopy **42–44**, 115 (1992).
[36] M. Böhringer, W.-D. Schneider, R. Berndt, K. Glöckler, M. Sokolowski, and E. Umbach, Phys. Rev. B **57**, 4081 (1998).
[37] While Böhringer *et al.* (Ref. 36) described the phenomenon of trapping molecules from a gas of mobile molecules on a metal surface, we believe that mobile molecules are likely to be present on closed molecular films as well. Furthermore, these authors showed that the trapping of molecules strongly depends on the tip-sample separation.